Verification of moisture budgets during drifting snow conditions in a cold wind tunnel

N. Wever,[1,2] M. Lehning,[1] A. Clifton,[1] J.-D. Rüedi,[1] K. Nishimura,[3,4] M. Nemoto,[3] S. Yamaguchi,[3] and A. Sato[3]

Received 14 October 2008; revised 30 March 2009; accepted 23 April 2009; published 25 July 2009.

[1] Experiments in a cold wind tunnel were used to verify drifting snow sublimation models. A layer of drifting snow particles was formed over a sintered snow surface. Sublimation and drifting snow flux were estimated from two vertically resolved profile measurements separated along the flow path and were compared to a simple, one-dimensional diffusion model of drift and drifting snow sublimation. The experiments show an increase in water vapor content of the air from drifting snow sublimation. The measured drifting snow sublimation appeared to be consistent with albeit somewhat larger than theoretical values found in the model study. Under wind tunnel conditions, particle number density appears to be the most important controlling factor on the sublimation rate. For experiments with external solar radiative forcing, the increase of the sublimation rate was also larger than theoretical predictions. The experiments suggest that irregular snow crystals and solar radiation might increase sublimation rates more than described by many drifting snow models.

Citation: Wever, N., M. Lehning, A. Clifton, J.-D. Rüedi, K. Nishimura, M. Nemoto, S. Yamaguchi, and A. Sato (2009), Verification of moisture budgets during drifting snow conditions in a cold wind tunnel, *Water Resour. Res.*, *45*, W07423, doi:10.1029/2008WR007522.

1. Introduction

[2] Sublimation is an important factor in the mass balance of snow surfaces. The sublimation may be altered by drifting snow, yet quantitative results on the exact magnitude of drifting snow sublimation and its effect on the local water balance and the moisture budget of the atmosphere have remained contradictory. Almost all drifting snow sublimation literature is based on extrapolating the experimental results by *Thorpe and Mason* [1966] for a single snow crystal to an ensemble of blowing snow particles. For instance, *Schmidt* [1982] has used this approach to calculate sublimation rates using measurements of particle size, particle number densities, humidity and temperature. He estimated the amount of sublimation during transport over 3 km to be about 39% of the transport rate for relative humidity values over ice of about 90%. In model studies for Arctic Alaska, 22% of the winter precipitation is estimated to return to the atmosphere as water vapor by means of drifting snow sublimation [*Liston and Sturm*, 1998]. Other drifting snow models give values ranging from 10% for Halley Station on an Antarctic ice shelf to 41% in the Canadian Prairies [*Bowling et al.*, 2004]. The discrepancy comes from the fact that moisture feedback effects in the atmospheric boundary layer (ABL) are difficult to assess and that simplified descriptions of airborne grain characteristics are used. Moisture, temperature and thus atmospheric stability effects of sublimating blowing snow have in detail been investigated by *Déry et al.* [1998]. There are two potential limits on the sublimation of drifting snow. The first limit is from the capacity of the ABL to remove saturated air from the drifting snow layer. Quick local saturation in the ABL may result in an only limited effect of drifting snow sublimation on the moisture budget of a snow surface. The second limit comes from the maximum moisture transport across the snow surface itself, which is mainly governed by the available energy. If this is the determining limit, drifting snow will significantly enhance sublimation.

[3] In this paper, we therefore try to investigate sublimation of an ensemble of blowing snow particles by wind tunnel measurements and model analyses. Because moisture budget measurements are difficult to perform in the field, we use wind tunnel moisture budgets to validate theoretical predictions of single grain sublimation and boundary layer feedback. To this end, we model single grain mass and energy exchange and incorporate the cumulative effect of the whole drifting snow grain population on the air moisture and energy budget using a simple one-dimensional turbulence model.

2. Theory

[4] The sublimation rate of a single grain can be calculated using two coupled equations for respectively heat and mass transfer between a particle and the surrounding air.

[1]WSL Swiss Federal Institute for Snow and Avalanche Research, Davos, Switzerland.
[2]Now at Royal Netherlands Meteorological Institute, De Bilt, Netherlands.
[3]Snow and Ice Research Center, National Research Institute for Earth Science and Disaster Prevention, Nagaoka, Japan.
[4]Now at Department of Environmental Science, Faculty of Science, Niigata University, Niigata, Japan.

0043-1397/09/2008WR007522

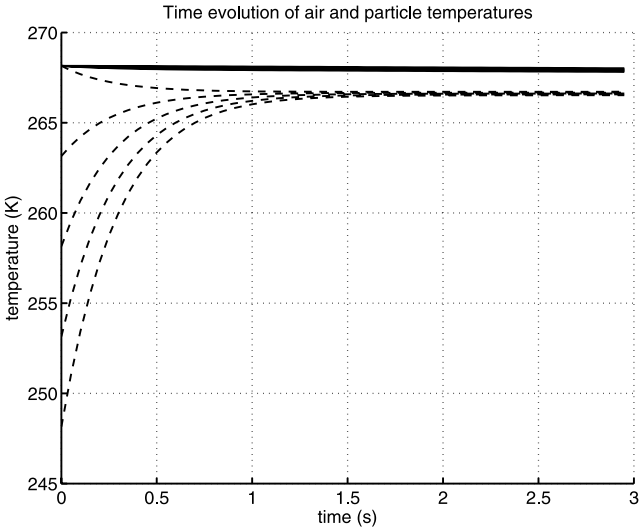

Figure 1. Time evolution of air temperature (solid lines) and particle temperature (dashed lines) for various initial particle temperatures (−25°C, −20°C, −15°C, −10°C, and −5°C). For each simulation, the initial air temperature was set to −5°C.

First, the heat transfer for a single ice particle surrounded by air is given by

$$c_{ice} m_p \frac{\mathrm{d}T_p}{\mathrm{d}t} = L_s \frac{\mathrm{d}m_p}{\mathrm{d}t} + S + 2\pi K_T r \left(T_{a,\infty} - T_p\right) Nu \ , \qquad (1)$$

where c_{ice} is the specific heat capacity of ice (J kg^{-1} K^{-1}), which is a function of temperature. m_p is the mass of the ice particle (kg), r is the radius of the particle (m), T_p is the temperature of the particle (K), S is the energy flow from an external source (for instance solar radiation) (J s^{-1}), K_T is the molecular thermal conductivity of the atmosphere (0.024 J m^{-1} s^{-1} K^{-1}), t is time (s) and L_s is the latent heat of sublimation of ice (2.838 × 10^6 J kg^{-1}). dm_p/dt is the mass change of a drifting snow particle due to sublimation (kg s^{-1}), $T_{a,\infty}$ is the temperature of the surrounding air (K) and Nu is the Nusselt number, which is a dimensionless measure of heat transfer. As either $T_{a,\infty} - T_p$ or dT_p/dt can be negative or positive, dm/dt can also be negative (mass loss) or positive (mass gain), indicating respectively sublimation or deposition.

[5] The mass balance for a single ice particle surrounded by air is given by

$$\frac{\mathrm{d}m_p}{\mathrm{d}t} + 2\pi D r \left(\rho_{w,r} - \rho_{w,\infty}\right) Sh = 0, \qquad (2)$$

where D is the diffusivity of water vapor in the air (m^2 s^{-1}) and $\rho_{w,r}$ is the water vapor density in the particle boundary layer (kg m^{-3}). $\rho_{w,\infty}$ is the water vapor density in the surrounding air (kg m^{-3}) and Sh is the Sherwood number, which is a dimensionless measure of mass transfer.

[6] The Nusselt and Sherwood numbers can be calculated using the approach by *Lee* [1975]:

$$Nu = Sh = \begin{cases} 1.79 + 0.606\sqrt{Re} & \text{for} \quad 0.7 < Re \le 10 \\ 1.88 + 0.580\sqrt{Re} & \text{for} \quad 10 < Re < 200 \end{cases}, \qquad (3)$$

where Re is the Reynolds number for falling particles, defined as the ratio of inertial to viscous forces acting on the particle:

$$Re = \frac{2 r V_v}{\nu}, \qquad (4)$$

where ν is the kinematic viscosity of air (1.3 × 10^{-5} m^2 s^{-1} for an air temperature of approximately 0°C). The ventilation velocity V_v is the relative speed of the snow particles to the air. It can be parameterized using a term for the terminal fall velocity and a term representing the enhanced ventilation of snow particles by turbulent eddies. We use a formulation by *Lee* [1975] which also takes this approach:

$$V_v = 1.1 \times 10^7 r^{1.8} + 7.5 \times 10^{-3} \left(\sqrt{2}\right) u^{1.36}, \qquad (5)$$

where u is the horizontal wind speed in the boundary layer at the height of the ice particle. This gives V_v = 5.3 m s^{-1} for a 100 μm particle in a 10 m s^{-1} wind.

[7] In most drifting snow literature [e.g., *Bintanja*, 2000; *Mann*, 1998; *Déry and Yau*, 1999; *Liston and Sturm*, 1998], sublimation rates of drifting snow particles are calculated using a thermal equilibrium approach for simplifying equations (1) and (2). We use the approach described by *Thorpe and Mason* [1966], assuming stationary conditions in the heat exchange between the sublimating snow particle and the air, which allows the particle mass change rate dm/dt to be calculated using

$$\frac{\mathrm{d}m}{\mathrm{d}t} = \frac{2\pi r \sigma - \dfrac{S}{K_T T_{a,\infty} Nu}\left(\dfrac{L_s M}{R T_{a,\infty}} - 1\right)}{\dfrac{L_s}{K_T T_{a,\infty} Nu}\left(\dfrac{L_s M}{R T_{a,\infty}} - 1\right) + \dfrac{1}{D \rho_s\left(T_{a,\infty}\right) Sh}}, \qquad (6)$$

where $\rho_s(T_{a,\infty})$ is the saturation density of water vapor at the temperature of the surrounding air, M the molecular weight of water (1.801 × 10^{-2} kg mol^{-1}), R the universal gas constant (8.313 J mol^{-1} K^{-1}) and σ denotes the water vapor deficit (undersaturation) with respect to ice, which is defined as

$$\sigma = \frac{\rho_{w,\infty}}{\rho_s\left(T_{a,\infty}\right)} - 1. \qquad (7)$$

Equation (6) is valid for conditions of thermal equilibrium. Then, changes in the particle temperature are negligible and all energy transferred to the particle drives sublimation. This assumption is only valid over a limited range of time scales, which can be estimated from explicit solutions to equations (1) and (2). We take representative conditions of a relative humidity over ice of 70%, an air temperature of −5°C, a particle radius of 3.0 × 10^{-4} m and zero external heat sources, such as incoming solar radiation. Nusselt and Sherwood numbers were calculated using a ventilation velocity of 5.3 m s^{-1}, which represents a wind speed of 10 m s^{-1} (equation (5)). Figure 1 shows the time development of air temperature and particle temperature for the first few seconds. It can be seen that even for large temperature differences between particles and the air, thermal equilibrium

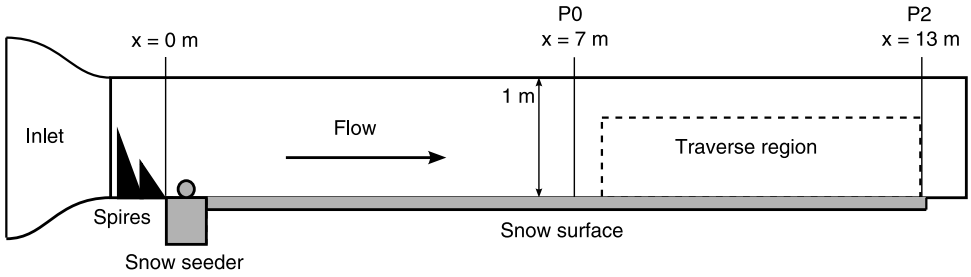

Figure 2. The working section of the Shinjo wind tunnel. Return section with fan and particle filters is not shown.

is reached within approximately 1 s. When modeling snow storms, the time scales of the modeled processes will generally be much larger than the time for the particles to reach equilibrium with air temperature.

3. Experiment Design

3.1. Wind Tunnel

[8] The experiments were carried out in the cryogenic wind tunnel of the Shinjo Branch of Snow and Ice Studies at the National Research Institute for Earth Science and Disaster Prevention in Shinjo, Japan. Figure 2 shows a schematic picture of the wind tunnel. The wind tunnel has been used for drifting snow investigations before and descriptions of the Shinjo facility can be found in work by *Kosugi et al.* [2004].

[9] The wind tunnel has a 13 m long, 1 m wide and 1 m high working section where the floor can be covered in snow. A snow seeder is installed upstream from the working section, and can be loaded with snow which is then fed into the wind tunnel flow. We used two discrete types of snow for seeding in the experiments reported here: (1) freshly made dendrites and (2) snow aged for several months at −15°C in a cold room. During this aging process, the snow crystals transform from dendritic shapes to rounded crystals. For both particle types, the snow seeder created asymmetrical particle size distributions that were skewed toward the small particle sizes. This is consistent with observations of particle size distributions during natural blowing snow events [*Gordon and Taylor*, 2009].

[10] The floor of the wind tunnel working section was covered with sieved snow which had been collected during the previous winter and allowed to age at −15°C. The snow was sprayed with water to sinter the surface. This surface was deliberately created so as not to release snow particles for saltation. Having snow drift over a snow surface resembles many natural conditions, although in real world situations, topographical features, the presence of vegetation and characteristics of the snow surface crystals can have an effect on the boundary layer different from our sintered wind tunnel surface.

[11] The wind tunnel is a closed system and the air was recirculated. In the recirculation path, a dehumidifier was installed, which allowed for an equilibrium between moisture added from the snow surface and from sublimating grains if present and the moisture extracted by the dehumidifier. This situation can be regarded as analogous to the situation in the atmospheric boundary layer, where a limited amount of moisture can be lost to the free troposphere. The curves in the recirculation path and the fan near the inlet completely destroy the boundary layer. Spires were located directly after the fan, designed to give a logarithmic profile boundary layer with a typical thickness of 0.5 m. The first 7 m of the wind tunnel working section were used to allow the buildup of a humidity boundary layer. This setup might result in partly developed boundary layers, giving a relatively low relative humidity close to the surface. Then, sublimation rates might be higher than found in typical natural conditions, where a fully developed boundary layer will be achieved during a long-lasting snow storm. The absence of a fully developed boundary layer in nature can be expected in, for instance, steep terrain.

[12] We installed two fixed vertical arrays of instruments 7 m and 13 m along the wind tunnel working section. These are known as P0 and P2, respectively. The space between those arrays will be referred to as test section. The characteristic travel times for the snow particles between the snow seeder and the upstream fixed profile vary between 0.6 and 0.9 s for the range of wind speeds used in our experiments. As the temperature difference between the particles and the air will be smaller than 10°C for this experimental setup, this time span will be sufficient to assume that the particles are in thermal equilibrium, as discussed above in section 2.

[13] At these fixed profiles, relative humidity and air temperature were measured at four heights, varying from approximately 2.5 cm to 30 cm above the snow surface. In addition, at 2.1 cm at the upstream profile and at 2.4 cm and 10.7 cm at the downstream profile, snow particle counters (SPCs) were installed. Dynamic pressure sensors were installed to measure wind speeds at 5.9 cm at the upstream profile and at 6.2 cm and 32.4 cm at the downstream profile. The wind tunnel has a mobile traversing system, which was equipped with a temperature and relative humidity sensor, an SPC and a wind speed sensor. The traverse was able to move between the two fixed profiles. The height of the sensors at the traverse could be varied from 2 cm to 50 cm above the surface. The traverse was used to obtain a more densely spaced vertical profile near the two fixed measurement arrays. Measurements using the traverse were made at discrete heights for approximately 20 s before moving on to the next height. The sampling frequency of all sensors was 1 Hz.

[14] Two types of combined temperature and humidity sensors were used on the fixed profiles: the HygroClip S3 and SC04 (manufactured by Rotronic AG), and the Handy Type RS-11 (manufactured by Tabai Espec Corporation). Table 1 lists the heights above the surface and types of the sensors mounted in the wind tunnel. The accuracy in water vapor density varied from 3.8% for the HygroClip S3 to 14.3% for the Handy Types. The traverse was equipped with a Vaisala HMP233 sensor, which has a nominal

Table 1. Temperature and Humidity Sensors[a]

	Profile		
Height (m)	P0	P2	Traverse
0.021	HC: SC04	-	
0.024	-	HC: SC04	
0.059	HT: RS-11	-	
0.062	-	HT: RS-11	
0.102	HT: RS-11	-	
0.107	-	HC: S3	
0.301	HT: RS-11	-	
0.324	-	HT: RS-11	
0.02–0.50			Vaisala: HMP233

[a]Locations and models of sensors used at the upstream (P0) and the downstream (P2) fixed profile and on the traverse. The height is measured as the distance from the surface to the center of the sensor. HT refers to Handy Type, and HC is HygroClip.

accuracy in water vapor density of 4.8%. All these values of accuracy are determined for reference situations as specified by the manufacturers. The SPC measures the number and size of particles passing through the detection volume and is calibrated to give an estimation of mass flux. The accuracy of the SPCs is not sufficient to measure the particle size decrease due to sublimation. The decrease of particle size between the two measurement arrays can be estimated to be less than 0.1% for typical particle sizes used in the experiments, while the relative width of the size classes used by the SPCs ranged from approximately 32% for the smallest to 3% for the largest particle sizes.

[15] The wind tunnel was also equipped with a solar simulator that simulated a shortwave radiation flux with at the surface a maximum of approximately 950 W m^{-2} along the center line of the test section when in use. This value is typical for midday in spring in the European Alps (e.g., at station Weissfluhjoch, daily maximum values of clear-sky shortwave downward radiation range from 400 W m^{-2} for December to 1080 W m^{-2} for June [*Marty*, 2000]). The solar simulator can therefore be regarded as a case of extreme sunshine. In nature, spring Föhn storms in the Alps often produce massive blowing snow clouds above ridges but not much deposition is observed in the lee. This would suggest that sublimation may be very important in these cases, which have not been investigated in detail, despite the fact that for drifting snow events during precipitation total mass transport over ridges has been successfully calculated without consideration of any sublimation effect [*Doorschot et al.*, 2001]. The solar simulator produced a spectrum comparable to sunlight and was used to study the influence of shortwave radiation on drifting snow sublimation.

[16] A series of nineteen experiments were carried out in the wind tunnel. As shown in Table 2, air temperature, wind speed, type of snow crystals and solar radiation (on/off) were varied. We divided the measurements into two time spans. A measurement series carried out while the traverse was measuring near the upstream profile is referred to as TR0, and near the downstream profile is referred to as TR2. Those time spans were approximately 3 min long each.

3.2. Sensor Calibration

[17] The experiments focus on the moisture budget in the wind tunnel, which can be determined by tracking changes in water vapor density. We used the temperature and humidity sensors to determine these changes. For this purpose, we calibrated the sensors with respect to water vapor density. For simplicity, only a linear offset compared to an arbitrarily defined reference sensor was determined. The HygroClip sensors were calibrated in a special calibration experiment in which all the sensors of this type were put next to each other under cold conditions. The Handy Type sensors on the fixed profiles were calibrated by comparing their readings to the traverse sensor when it was in the same vertical region. For this calibration procedure, we used experiments 5, 8, 15, 18 and 22. Those experiments did not have drifting snow conditions or extra radiative forcing by the solar simulator and therefore have little complex influences. The HygroClip sensor at 10.7 cm at the downstream profile was taken as the arbitrary reference sensor. Then, the offset of the sensor on the traverse was determined by taking the mean difference between the measurements from this reference sensor and the sensor at the traverse when the traverse was at equal height. Using the calibrated measurements from the traverse, the offsets of the other Handy Type sensors at the fixed profile were determined and corrected for. This procedure resulted in an accurate relative calibration, which was suitable for our mass balance analysis, where we only look at moisture differences. Table 3 shows the mean offset and standard deviation for each sensor used in the analysis of the experiments.

[18] The water vapor content of the air at the two profiles was determined by integration of the water vapor density from 0 to 40 cm above the surface, arbitrarily assuming a boundary layer depth of 40 cm in the tunnel. Integration

Table 2. List of the Various Experiments Carried Out in the Wind Tunnel, Showing the Different Setups and Steering Parameters for the Experiments[a]

Experiment Number	T_{inlet} (deg C)	U_{inlet} (m/s)	Seeding	Solar Simulator?
5	−15	10	-	-
6	−15	10	old snow	-
7	−15	8	old snow	-
8	−15	8	-	-
9	−15	5	-	-
10	−15	12	-	-
13	−15	12	old snow	-
14	−15	12	-	-
15	−15	8	-	-
16	−15	8	dendrites	-
17	−15	10	dendrites	-
18	−15	10	-	-
21	−15	10	old snow	-
19	−15	10	-	yes
20	−15	10	old snow	yes
22	−5	10	-	-
25	−5	10	old snow	-
23	−5	10	-	yes
24	−5	10	old snow	yes

[a]Experiments that can be compared are grouped (see text).

Table 3. Water Vapor Density Offsets for the Temperature and Humidity Sensors Relative to the Reference Sensor[a]

		Mean Offset						SD		
		Water Vapor Density ($\times 10^{-5}$ kg m^{-3})			Percentage (%)			Water Vapor Density ($\times 10^{-5}$ kg m^{-3})		
Sensor	Height (m)	P0	P2	TR	P0	P2	TR	P0	P2	TR
$P0_1$	0.021	17.0	-	-	15.2	-	-	5.3	-	-
$P2_1$	0.024	-	28.3	-	-	25.4	-	-	9.2	-
$P0_2$	0.059	−11.1	-	-	10.0	-	-	3.4	-	-
$P2_2$	0.062	-	29.1	-	-	26.1	-	-	19.8	-
$P0_3$	0.102	−5.6	-	-	5.0	-	-	2.9	-	-
$P2_3$	0.107	-	0	-	-	0	-	-	0	-
$P0_4$	0.301	−7.4	-	-	6.6	-	-	4.8	-	-
$P2_4$	0.324	-	−10.3	-	-	9.2	-	-	6.4	-
TR	traverse	-	-	1.9	-	-	1.7	-	-	1.3

[a]For sensor details, see Table 1. The offset (kg m^{-3}) is the mean for all experiments, relative to the HygroClip at 0.107 m on P2. The percentage is the offset as a percentage of the water vapor density at −15°C and 70% relative humidity, which is 1.115×10^{-3} kg m^{-3}. This reference case applies to four of the five calibration experiments. SD is the standard deviation between experiments.

was carried out by approximating the true profile by linear interpolation in between the measurement points and the surface, which was assumed to be saturated. Above the highest measurement point, a constant profile was assumed. The main analysis of the wind tunnel data focused on the change in water vapor content between the two measurement arrays. When there is no drifting snow, we assume that the change in water vapor content in the wind tunnel is due to sublimation of water vapor from or deposition onto the snow surface. When drifting snow is present in the wind tunnel, we assume that we have both the mass exchange with the surface as well as the sublimation of the drifting snow particles. The experiments were designed so that each experiment which had drifting snow was comparable to an experiment under similar conditions, but without drifting snow. We will define a so-called drifting snow sublimation effect, which is the change in water vapor content for the experiment with drifting snow minus the change in water vapor content for the experiment without drifting snow. The drifting snow sublimation effect then is the extra change in water vapor content by sublimation of the drifting snow.

[19] In experiments 9, 10 and 14, the temperature and relative humidity sensor at the highest position at the downstream profile was not functioning. Because this measurement level contains the information about a large part of the boundary layer, we decided to discard the corresponding experiments from the analysis. In experiments 13, 15, 16 and 17, the sensor 0.107 m above the surface at the downstream profile was not functioning. Data from these experiments were included in the analysis, because the absence of the measurements by this sensor only introduced a marginal error. We estimate that the integration procedure overestimates the water vapor density at the level of the missing records with approximately $2–3 \times 10^{-5}$ kg m^{-3}, compared to experiments with correct working sensors. Because the sensor at that height is representing approximately 4 cm (half the distance between the sensor above and below the faulty sensor), linear interpolation will give a change in water vapor content which is approximately $0.8–1.2 \times 10^{-6}$ kg m^{-2} too large. For the drifting snow sublimation effect of experiment 16, which was compared to experiment 15, this overestimation will for a large part cancel out, as the linear interpolation for the broken sensor was applied on both experiments. For the comparison of experiment 17 and 18, we are likely to overestimate the sublimation effect in experiment 17 with approximately $0.8–1.2 \times 10^{-6}$ kg m^{-2}, because only in experiment 17 linear interpolation for the broken sensor was applied.

[20] Usually, the wind tunnel was run for 15 min before the start of an experiment to achieve equilibrium conditions. Equilibrium was taken to mean changes in air temperature and humidity of less than 1°C and 10% relative humidity over ice in those 15 min. During experiments with drifting snow, quasi-equilibrium could be reached as moisture was constantly removed from the air in the tunnel by a dehumidifier, compensating for the sublimation from the snow and snow surface. Occasional maintenance in the tunnel between experiments apparently disturbed the equilibrium, and the TR0 measurements in experiments 6, 7 and 24 were later found not to be in equilibrium, shown by a large relative humidity increase (over 5%), and so were neglected. We also had an experimental plan that attempted to put experiments, which should be compared to each other, as closely together (in time) as possible.

[21] Attempts to measure the mass change of the snow layer covering the wind tunnel floor with a balance in the floor of the wind tunnel were not successful. The dynamic pressure fluctuations in the wind tunnel appeared to disturb the measurements too much. Therefore, we could not explicitly measure the sublimation from or deposition onto the snow surface.

4. Modeling

[22] The experiments in the wind tunnel are modeled using a 1 dimensional turbulence model. This turbulence model solves the governing equations for humidity and potential temperature, using first-order closure for the turbulent fluxes. The model simulates the development of humidity and potential temperature of a column of air when it travels between the two fixed profiles. It was applied on the various experiments performed in the wind tunnel, with a focus on the TR2 time periods. The data set for this time period is more robust.

[23] The governing equation for specific humidity is [*Stull*, 1989]

$$\frac{\partial q}{\partial t} = -\frac{\partial \overline{w'q'}}{\partial z} - \frac{1}{(\rho_d + \rho_w + \rho_{ds})} q_{ds}, \tag{8}$$

where q is the specific humidity (kg kg^{-1}), $\overline{w'q'}$ is the turbulent moisture flux (m kg s^{-1}), z is the vertical coordinate (m), ρ_d is the density of dry air (kg m^{-3}), ρ_w is the density of water vapor (kg m^{-3}), ρ_{ds} is the density of the water vapor originating from drifting snow sublimation (kg m^{-3}), and q_{ds} is the local sublimation rate (kg m^{-3} s^{-1}).

[24] The governing equation for potential temperature is

$$\frac{\partial \theta}{\partial t} = -\frac{\partial \overline{w'\theta'}}{\partial z} + \frac{L_s}{(c_{p,d}\rho_d + c_{p,w}\rho_w + c_{ice}m_{ds})} q_{ds}, \tag{9}$$

where θ is the potential temperature of the air (K), $\overline{w'\theta'}$ is the turbulent heat flux (m K s^{-1}), $c_{p,d}$ is the specific heat capacity of dry air (J kg^{-1} K^{-1}), $c_{p,w}$ is the specific heat capacity of water vapor (J kg^{-1} K^{-1}) and m_{ds} is the concentration of ice particles (kg m^{-3}).

[25] The equations for moisture and heat were solved using an explicit scheme. An Euler forward scheme was used to solve the time derivatives. The spatial derivatives were solved using central differences. The model domain consisted of 81 nodes, each 0.5 cm apart, extending from the surface to 40 cm above the surface.

[26] To integrate the model over the domain of the wind tunnel test section, we invoked Taylor's hypothesis. This means that we assumed the advection of the turbulent fields through the test section to be dominated by the mean flow. We have expressed for each grid cell the time integration steps as spatial steps using wind speed, so we were able to perform a spatial integration over the distance between the two sensor arrays:

$$\Delta t = \frac{\Delta x}{u}, \tag{10}$$

where Δt is the model time step at the grid cell (s), Δx is the spatial step in the model (m) and u is the wind speed at the grid cell (m s^{-1}).

[27] Initial temperature and humidity profiles for the model were determined from the upstream profile P0. From the surface to the highest measurement point, these profiles were linearly interpolated and extrapolated onto the model grid. At the surface, the air was assumed to be saturated. Above the highest measurement point, the humidity and temperature profiles were kept constant with height. Boundary conditions were chosen accordingly. At the surface, Dirichlet boundary conditions were used, keeping the surface saturated and at initial temperature. As we observed no clear signal of a temperature change at the surface, we decided to neglect a possible temperature decrease of the surface due to surface sublimation, which can be expected to be small. At the upper boundary, Neumann boundary conditions were chosen, keeping the flux of heat and moisture across the upper boundary constant. Because the gradients were forced to zero, no moisture or heat was transported through the upper boundary. The profiles for humidity show a strong increase in humidity close to the surface. The air temperature varied only about 0.5°C with height.

[28] The model was used to simulate the conditions during the TR2 period (traverse in the downstream position). Recall that we assume stationarity in the tunnel test section, an assumption, which is in reality better fulfilled at the end of the test section. Because snow particle concentration varied strongly over the course of the experiment, initial drifting snow concentration and particle radius profiles were obtained from the traverse SPC data, while it was measuring near the downstream profile P2. The particle concentration and radius decrease due to sublimation from P0 were smaller than can be measured by the SPC and the error introduced by taking the P2 concentration and radius profile can safely be neglected.

[29] The model describes overall sublimation from all particles by assuming a single mean effective radius. The effective radius is approximated by the area-weighted mean particle radius, derived from the ensemble of 32 size classes as measured by the SPC. The amount of drifting snow sublimation was calculated by multiplying the sublimation rate for a single grain with mean effective radius (equation (6)) with the particle number density, getting the same local sublimation rate as when the measured ensemble from the SPC would have been used.

[30] We assumed a fully developed boundary layer with a roughness length z_0 of 0.1 mm and calculated the friction velocity u_* from the velocity measured by the traverse at 0.3 m, assuming a log law relationship. These values of u_* and z_0 were then used to generate a boundary layer velocity profile from the log law.

[31] The effect of solar radiation is not included in the model. Although this could be included in equation (1) and has been used in models by, e.g., *Liston and Sturm* [1998], the effect is difficult to assess because of an uncertainty in the determination of the particle albedo. As the particles are ice, the albedo may be expected to be high, but any surface structure or scarring from impacts may also decrease the albedo. Following *Liston and Sturm* [1998], sublimation rates for particles exposed to a downward shortwave radiation flux of 950 W m^{-2} will increase by approximately 15% for typical conditions in the wind tunnel (i.e., a relative humidity over ice of 70%, an air temperature of −15°C, a particle radius of 3.0×10^{-4} m and a Nusselt number of 10).

[32] The turbulent moisture and temperature fluxes were computed using a first-order closure scheme, parameterizing the moisture and temperature flux by the gradient, scaled by the eddy coefficient:

$$-\overline{X'w'} = K\frac{\partial X}{\partial z}, \tag{11}$$

where X is a physical quantity and K is the eddy diffusion coefficient for quantity X (m^2 s^{-1}). A common parameterization for the eddy coefficient for a neutral surface layer is given by the Prandtl mixing length approach [*Stull*, 1989]

$$K = \kappa^2 z^2 \sqrt{\left(\frac{\partial u}{\partial z}\right)}, \tag{12}$$

where K is the eddy coefficient (m^2 s^{-1}), taken the same for both moisture and temperature, and κ is the von Kármán constant (0.4).

[33] The eddy coefficients were scaled with a constant (C), so that the latent heat flux from the surface in the mixing model resulted in an equal change in water vapor content as in experiments without drifting snow. The calculation of C from the profiles can be seen equivalent to determining the (moisture) roughness length in a typical Monin-Obukhov surface layer parameterization.

[34] The latent heat flux in the model was calculated using the flux profile relation for a neutral boundary layer:

$$Q_L = -\rho_{air} L_s K \frac{\partial q}{\partial z}, \tag{13}$$

where Q_L is the latent heat flux (J m^{-2} s^{-1}).

Table 4. Changes in Water Vapor Content During Experiments[a]

Experiment Number	Change in Water Vapor Content ($\times 10^{-5}$ kg m^{-2})		
	During TR0	During TR2	Mean
5	1.16	0.61	0.89
6	-	1.54	1.54
7	-	1.05	1.05
8	0.22	0.71	0.46
13	0.16	2.74	2.18
15	1.16	1.50	1.33
16	2.61	3.06	2.83
17	2.45	2.49	2.47
18	0.43	0.23	0.33
21	2.49	2.16	2.32
19	0.98	1.23	1.11
20	5.23	3.38	4.30
22	−1.62	−2.09	−1.85
25	0.48	−1.07	−2.94
23	−2.40	−2.03	−2.22
24	-	1.17	1.17

[a]Values given are the integral between 0 and 40 cm above the surface. Experiments that can be compared are grouped (see text). In experiments 9, 10 and 14, the temperature and relative humidity sensor at the highest position at the downstream profile was not functioning. Because this measurement level contains the information about a large part of the boundary layer, we decided to discard the corresponding experiments from the analysis.

[35] The latent heat flux at the surface in the wind tunnel can be related to the change in water vapor content between the two fixed profiles:

$$Q_L = \Delta\epsilon_w L_s \frac{U}{\Delta X}, \tag{14}$$

where $\Delta\varepsilon_w$ is the change in water vapor content (kg m^{-2}), ΔX is the distance between the two fixed profiles, in this case 6 m. U is the depth-averaged wind speed in the air layer influenced by the moisture transport from the surface.

[36] The numerical model simulates the latent heat flux from the surface by calculating the latent heat flux between the surface layer and the first layer above the surface. After substituting the numerical discretizations for the latent heat flux for the surface layer and the numerical approximation of the logarithmic wind profile at the first grid point above the surface, we can express the constant C as

$$C = \frac{-12\Delta\epsilon_w}{5\rho_{air}\kappa^2\Delta x\Delta z\frac{dq}{dz}}, \tag{15}$$

where dq/dz represents the humidity gradient at the surface, which can be approximated in the model by the gradient between the surface and the first grid point.

[37] The value of C was calculated for each experiment without drifting snow. The same value for C was then used for modeling the comparable experiment with drifting snow. Using this procedure, we were able to reproduce approximately the same change in water vapor content as measured for an experiment without drifting snow. This approach resulted in values for C between 0.13 and 0.84. We think that the variability in the values for C stems from different surface roughnesses between the experiments and from measurement errors. This variability will only slightly influence the results, as the experiments that will be compared to each other were assumed to have equal values for C.

5. Results and Discussion

5.1. Experiment Results

[38] Table 4 shows the measured changes in water vapor content between the upstream and downstream profiles. Table 5 shows the experiments with drifting snow and the experiments they can be compared to on the basis of temperature, wind speed and whether the solar simulator was in use. Table 5 also shows the drifting snow sublimation effect as defined in section 3.2. The change in water vapor content between the two profiles was larger when the snow seeders were used and snow was drifting in the tunnel. The increase in water vapor content compared to experiments without drift is considerable. It is between 1.5 and 10 times higher, much larger than the accuracy of the sensors. As discussed earlier, we are likely to overestimate the drifting snow sublimation effect for experiment 17, but Table 5 shows that the overestimation is much smaller than the drifting snow sublimation effect.

[39] Experiments carried out at a temperature of approximately −15°C show a positive change in water vapor content for both the TR0 and TR2 time spans. On the contrary, the experiments carried out at −5°C, show a much smaller and sometimes even a negative change in water vapor content. This suggests that water vapor is being

Table 5. Drifting Snow Sublimation Effect Determined by Comparing Experiments Without Drifting Snow to Experiments With Drifting Snow[a]

Experiment Number		Drifting Snow Sublimation Effect ($\times 10^{-5}$ kg m^{-2})		
No Drift	With Drift	TR0	TR2	Mean
5	6	-	0.926	0.926
8	7	-	0.346	0.346
15	7	-	(−0.448)	
13	-	-	-	-
8	16	(2.40)	(2.35)	
15	16	1.45	1.55	1.50
18	17	2.02	2.26	2.14
19	20	4.25	2.14	3.19
5	21	(1.33)	(1.55)	
18	21	2.06	1.93	2.00
23	24	-	3.20	3.20
22	25	2.10	1.02	1.56

[a]Drifting snow sublimation effect is shown for both TR0 and TR2 time spans when possible. The mean value is given as the mean of both time spans, when applicable. Some experiment comparisons are probably not fair for other reasons, as described in the text. These comparisons are denoted by values in parentheses.

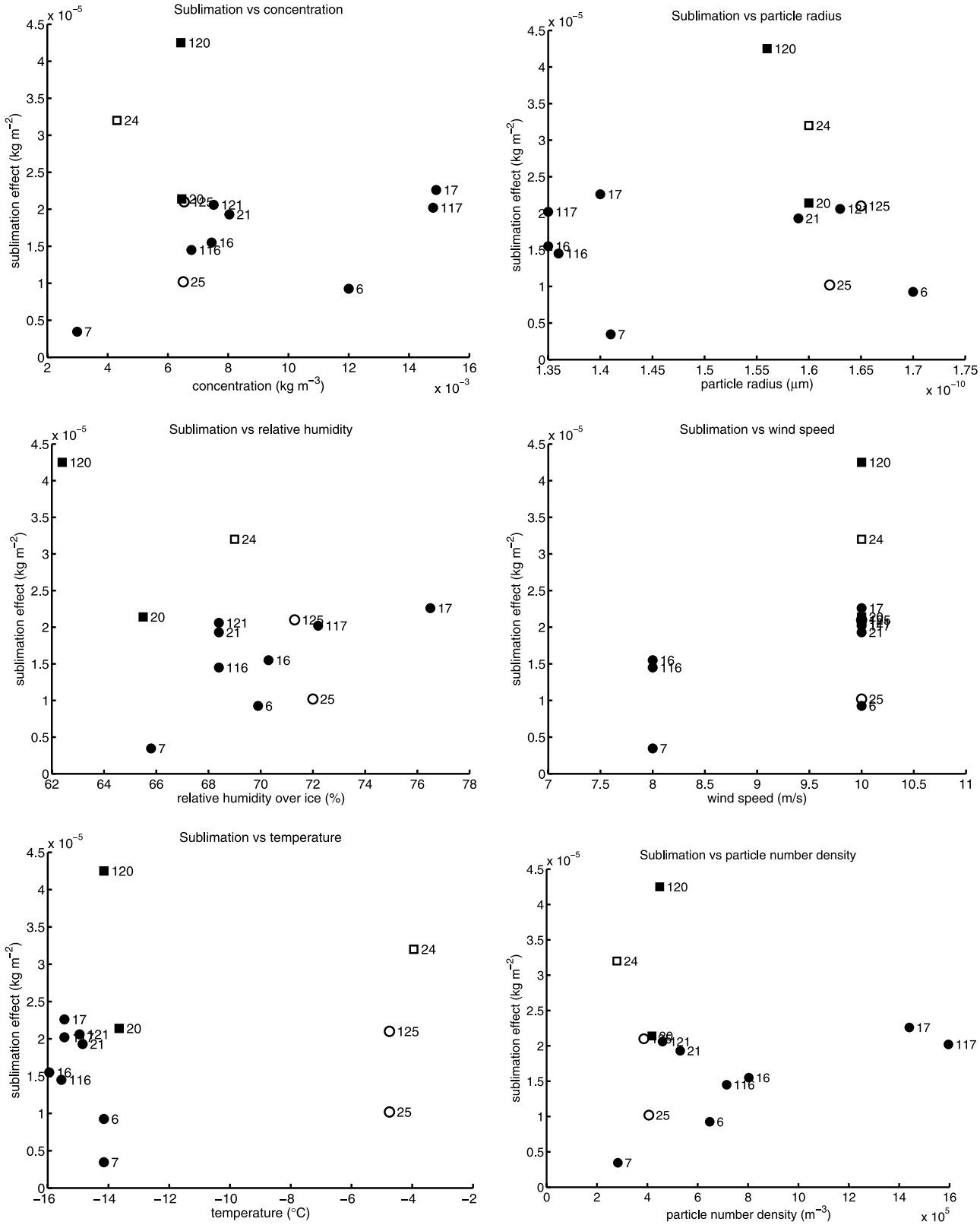

Figure 3. Drifting snow sublimation effect of the various experiments against (top left) height-averaged concentration, (top right) particle radius, (middle left) relative humidity over ice, (middle right) wind speed, (bottom left) height-averaged temperature, and (bottom right) particle number density, calculated from radius and concentration. Both experiments at −15°C (solid markers) and −5°C (open markers) are shown. Experiments with the solar simulator on are denoted by squares instead of circles. Numbers smaller than 100 denote the TR2 time span. For the TR0 time span, experiment numbers are preceded by a 1.

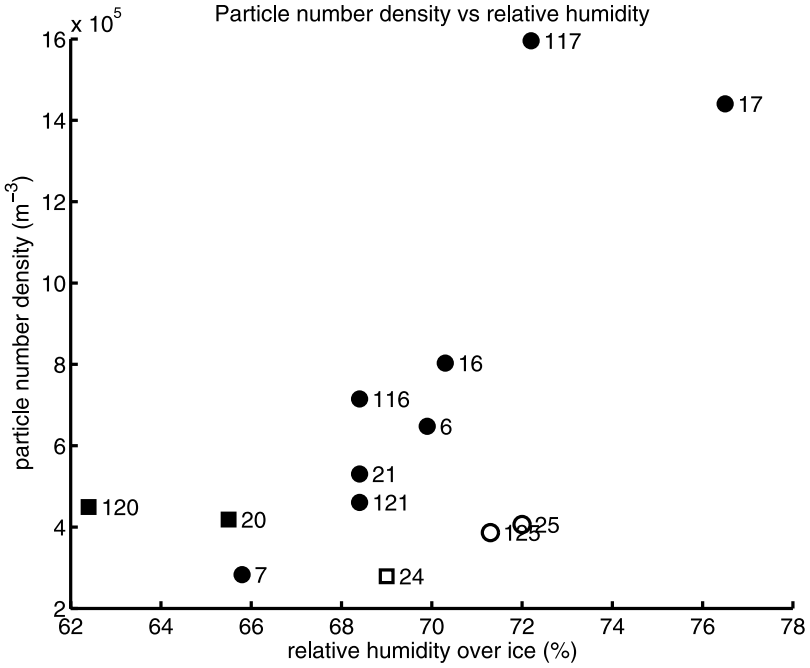

Figure 4. Number density of drifting snow particles against the height-averaged relative humidity over ice in the wind tunnel. For a description of the markers, see the caption of Figure 3.

deposited on the surface; the experiments at −5°C were carried out a few hours after the experiment series at −15°C, and so it is possible that the snow surface or other wind tunnel parts were still colder than the air. Measurements of the snow surface temperatures were made, but postprocessing of the data showed them to be unusable and so we cannot verify this hypothesis.

[40] Although the experiments covered a range of conditions with regard to air temperature, snow seeding and solar radiation (as described in Table 2), the range of conditions sampled and the total number of experiments was too small, to isolate individual effects, with the exception of solar radiation. The experiments with solar radiative forcing show a larger drifting snow sublimation effect than the other experiments. Figure 3 shows the measured drifting snow sublimation effect as a function of concentration, particle size, relative humidity, wind speed, temperature and particle number density. We can see that almost no correlation is present between measured drifting snow sublimation effect and the particle radius, temperature and wind speed. An explanation is that the range over which those variables varied during the experiments is so small that the effect on sublimation rate is smaller than what we could detect with our setup. The possible temperature decrease caused by sublimation of drifting snow [*Déry et al.*, 1998], is not confirmed in the experiments because of the limited fetch.

[41] Figure 3 shows a weak positive correlation between concentration and drifting snow sublimation effect. A stronger correlation can be seen in the particle number density versus sublimation effect (bottom right plot in Figure 3), although it is for a large part determined by experiment 17. This correlation is expected, because a higher particle number density means more particles which can sublime. This significantly increases the amount of moisture added to the air.

[42] There are three factors that may be disturbing this correlation. First, experiments 20 and 24 show a relatively large sublimation effect, although particle number densities are low. Interestingly, those points represent experiments with solar radiation, suggesting that solar radiation can increase sublimation significantly. This will be discussed later. Another part of variation in sublimation rate can be explained by changes in humidity and temperature. A positive correlation between relative humidity and drifting snow sublimation effect was found, which is in contradiction to equation (6). However, we also find a positive correlation between relative humidity and particle number density (see Figure 4). This indicates that during the experiments in the wind tunnel, the higher the particle number density, the higher the relative humidity. This is due to the fact that the total sublimation rate increases with increasing particle number density, causing the air to become more humid. According to equation (6), the sublimation rate scales linearly with undersaturation. By using this linear relationship, we can correct the measured sublimation effect as if all experiments were carried out at a relative humidity of 69%. Temperature also influences the sublimation rate. Using equation (6), it can be shown that the sublimation rate at −15°C is approximately 0.51 times the sublimation rate at −5°C, independent of relative humidity and particle size. When we correct for both humidity and temperature, the correlation between particle number density and drifting snow sublimation effect increases (see Figure 5). Neglecting the experiments with solar radiation, the R^2 value for the linear correlation (based on 10 points) increases from 0.25 for the uncorrected measurements to 0.58 for the temperature and relative humidity corrected measurements.

[43] Figure 5 illustrates the important effect of particle number density in determining the sublimation rate. It appears to be more important than particle radius or mass concentration. For instance, experiment 6 had high values of

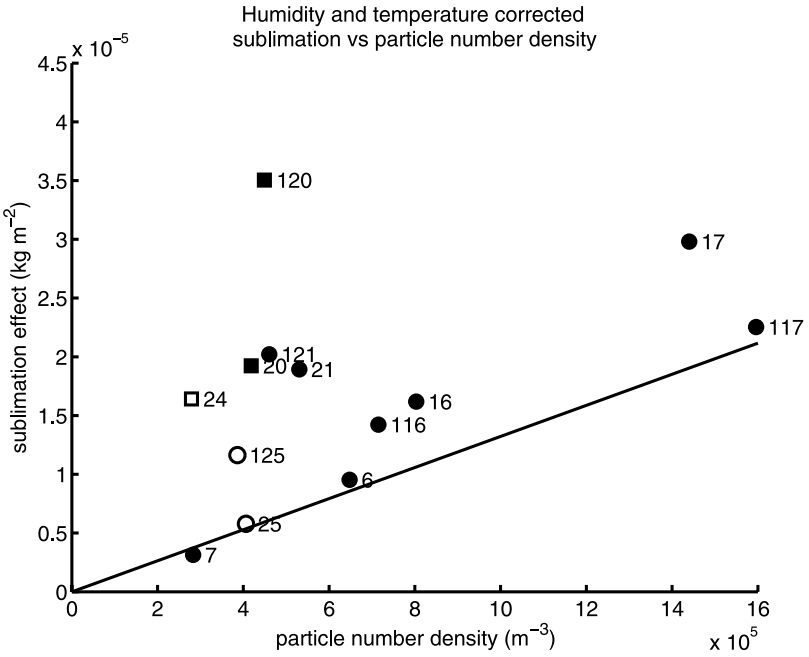

Figure 5. Drifting snow sublimation effect against the particle number density of drifting snow particles in the wind tunnel. The sublimation effect is corrected to a relative humidity of 69% and a temperature of −15°C (see text). For a description of the markers, see the caption of Figure 3. The solid line shows a theoretical relationship between particle number density and drifting snow sublimation effect.

concentration, but because of large particle sizes, it had relatively low particle number densities, resulting in lower sublimation rates. Increasing the particle number density while holding the mass concentration constant increases the sublimation rate more than is compensated for by a decreasing single grain sublimation rate belonging to a smaller particle radius. As the particle number density is the dominating factor in the total drifting snow sublimation, attention should be paid getting accurate particle number densities when initializing models for simulating drifting snow events. This could require using more accurate models of the surface conditions, as described by *Clifton and Lehning* [2008].

[44] To compare the measured sublimation effect to theoretical values provided by equation (6), a theoretical prediction of the relationship between particle number density and sublimation effect for typical conditions found in the wind tunnel experiments is shown in Figure 5 (solid line). As can be seen, the sublimation effect for a given particle number density is higher than theoretical values. Such an underestimation is also seen in the model results below.

5.2. Model Results

[45] Table 6 shows the modeled change in water vapor content and the total amount of drifting snow sublimation,

Table 6. Results of the Model Simulations of the Wind Tunnel Experiments[a]

Experiment Number	Modeled Change in Water Vapor Content ($\times 10^{-5}$ kg m^{-2})	Drifting Snow Sublimation Effect		
		Modeled ($\times 10^{-5}$ kg m^{-2})	Measured ($\times 10^{-5}$ kg m^{-2})	Ratio Measured Over Modeled
5	0.629	-		
6	1.33	0.756	0.926	1.22
7	0.945	0.273	0.346	1.27
8	0.707	-		
13	2.31	0.151	-	
15	1.29	-		
16	1.96	0.684	1.55	2.27
17	1.18	0.954	2.26	2.37
18	0.302	-		
19	1.41	-		
20	2.13	0.566	2.14	3.78
21	0.877	0.609	1.93	3.16

[a]The modeled change in water vapor content is determined from the difference between the initial profile and the modeled downstream profile. The modeled drifting snow sublimation effect is the total sublimation during the model simulation as given by equation (6). The measured TR2 drifting snow sublimation effect from Table 5 is shown for easy comparison. The ratio denotes the ratio between measured and modeled drifting snow sublimation effect.

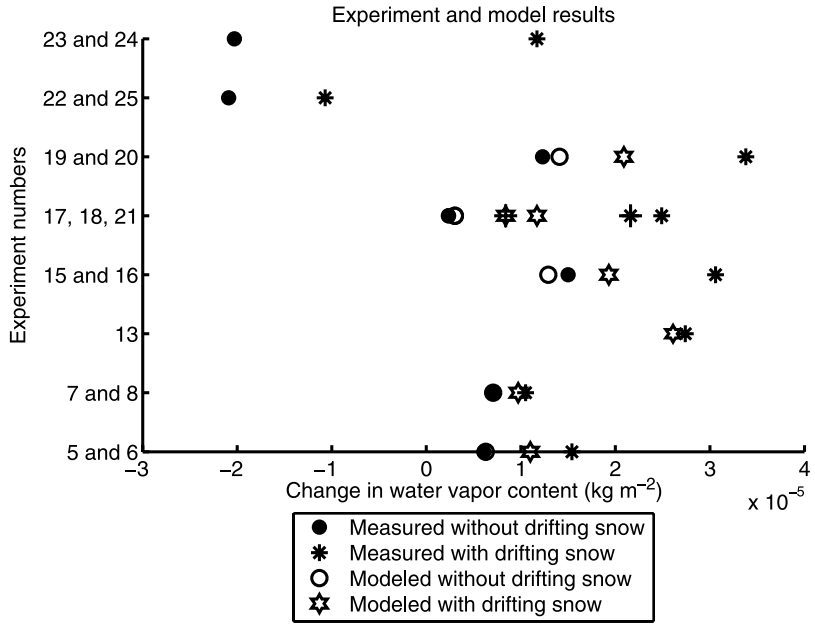

Figure 6. Comparison of model results (open markers) and measurements (solid markers) for the wind tunnel experiments for the TR2 time period. At each horizontal line, experiments are shown which are comparable (for details, see Table 5). Circles denote experiments without drifting snow, and stars denote experiments with drifting snow. Note that the one case in which three experiments were comparable (experiments 17, 18, and 21), the two different experiments with snow drift can be distinguished by a slightly different marker. For the experiments at −5°C, no simulations were done.

calculated using equation (6). Figure 6 graphically represents both the measured and modeled results. The model was applied only on experiments carried out at −15°C, because the possible occurrence of deposition on the surface in experiments at −5°C made it impossible to initialize the model the same way as for the other experiments.

[46] The model results confirm the increase in moisture content of the air when there is drifting snow present, as found in the measurements. As we can see, the change in water vapor content between the inlet (P0) and outlet (P2) of the wind tunnel is larger in experiments and model simulations with drifting snow than without drifting snow.

[47] Figure 7 shows an example of measured and modeled profiles for an experiment without drifting snow (experiment 19) and the comparable experiment with drifting snow (experiment 20). As can be seen, modeled and

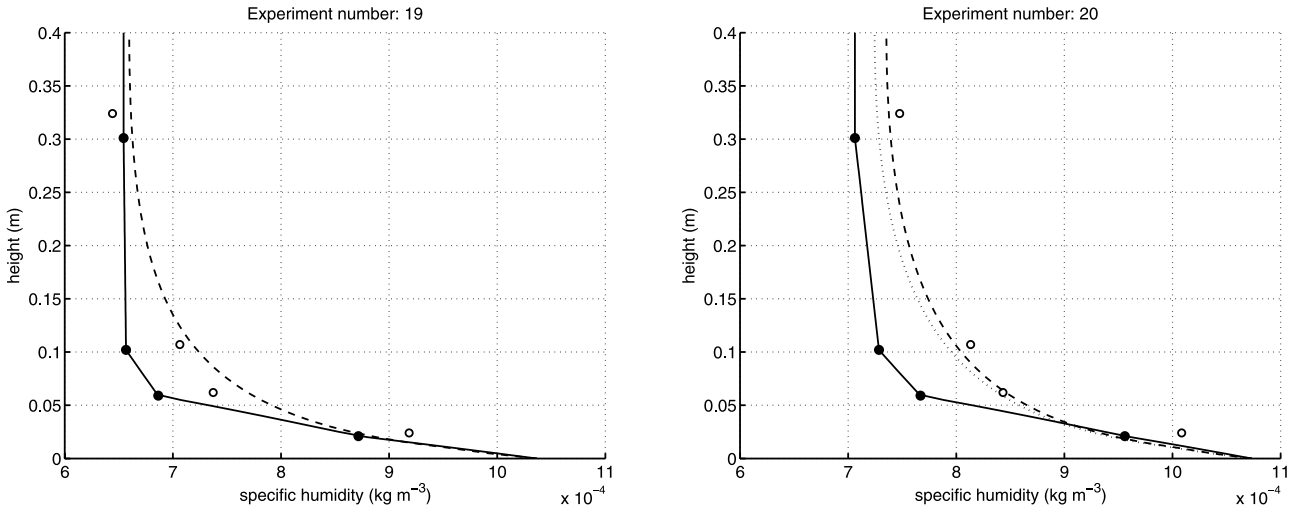

Figure 7. Measured and modeled specific humidity profiles for (left) experiment 19 and (right) experiment 20. The measured profiles are indicated by the circles. Both upstream (solid circles, solid line) and downstream (open circles, dashed line) profiles are shown, averaged over the TR2 time span. For experiment 20, the modeled downstream profile including drifting snow sublimation is shown (dashed line). For comparison, the model was also run with the same initial conditions but without modeling drifting snow sublimation (dotted line).

measured profiles are in quite good agreement for the two experiments shown here. More important, Figure 7 clarifies how drifting snow sublimation changes the humidity profiles in the model.

[48] The ratio between modeled and measured drifting snow sublimation shows that the model consistently underestimates the drifting snow sublimation. The most likely reason for this is an underestimation of the snow particle density by the SPCs. The SPCs are very difficult to calibrate and were used without recalibration, which may have been a problem [*Clifton et al.*, 2006]. Because the sublimation rate is very sensitive to particle number density, this can contribute to the difference between measured and modeled drifting snow sublimation effect. Another cause may be the model assumption that the snow particles are perfect spheres, as in reality they will have all kind of irregular shapes. Because the ratio of area to volume for a sphere is the lowest possible for a three-dimensional shape, the sublimation rate of a perfect sphere will be smaller than any other shape with the same mass. Moreover, irregular shapes of the blowing snow particles will alter the terminal fall and ventilation velocities, affecting sublimation rates as well. For calculating sublimation rates of nonspherical snow particles, we can use the results of experiments with natural snow crystals of dendritic stellar variety by *Thorpe and Mason* [1966], on the basis of the work on shape factors for snow crystals by *McDonald* [1963]. Although it is hard to compare the sublimation rate of a perfect sphere to the sublimation rate of a dendritic snow crystal because of large differences in volume and radius, the effect of having a complex particle shape is illustrated by the result of *Thorpe and Mason* [1966], that the efficiency of the mass and energy exchange increases a factor 2.5 to 5 for dendritic shapes, compared to hexagonal plates. The highest sublimation rates are observed with crystals composed of very fine branches. We can conclude that the model will underestimate the sublimation rate when it assumes the particles to be perfect spheres. We would then expect to see this reflected in the measurements: the drifting snow sublimation effect should be larger for dendritic snow than for old snow. Although this is seen for the two experiments with dendritic snow compared to the first two experiments with old snow, it is the opposite for the last two experiments with old snow. We did not find an explanation for this.

[49] An other source of model uncertainty is the roughness length of the surface. We assumed a typical value of 0.1 mm, which is consistent with similar wind tunnel studies [*Clifton et al.*, 2006]. It is known that roughness lengths vary significantly dependent on the presence of snow drift and the shape of the drifting snow crystals. Lower roughness values will give a shorter residence time for particles in the wind tunnel, but an increased ventilation velocity. A model sensitivity study for z_0, showed approximately 2% less snow drift sublimation if roughness was assumed to be 1 order of magnitude lower, while total change in water vapor content between inlet and outlet decreased by approximately 8% for this lower roughness. This means that when using a smaller roughness length, the model would underestimate the snow drift sublimation even more compared to the measurements. Higher assumed roughness lengths would lead to larger changes (not shown) but become unrealistic [*Clifton et al.*, 2006].

5.3. Solar Radiation

[50] Experiments show a stronger drifting snow sublimation effect when there is an additional forcing by solar radiation, than without. Interestingly, the effect of solar radiation appears to be much stronger than the theoretical prediction of an increase of about 15% (section 4). However, the drifting snow sublimation effect in the experiments is about 50% higher with radiation than without. The possibility that the measurements were disturbed by heating of the instruments by the solar simulator is limited by the fact that we looked at water vapor density, which is not influenced by temperature. Moreover, when the measurements of the temperature and humidity sensors were disturbed by the solar simulator, this effect would be higher on the highest sensor. However, comparing experiment 19 and 20 (see Figure 7), we see that the behavior of the highest sensor agrees with the model results. The large increase of humidity registered by the highest sensor in experiment 20 can be explained by larger concentrations of snow particles at higher levels in the wind tunnel than seen in the other experiments. Therefore, heating of the instruments cannot fully explain the effect observed.

[51] Another possible explanation for the higher solar influence on sublimation rates may be again that the particles are irregular in shape, having a larger surface area to volume ratio. That will generally increase the effect of incident solar radiation. However, we would also think that the solar simulator lamps heated the wind tunnel walls on all sides, thereby increasing the energy available locally for sublimation, since the walls will radiate and conduct heat back to the tunnel air. As a result, the Nusselt and Sherwood numbers are larger under solar radiation because of increased convective processes.

5.4. Latent Heat Flux

[52] The latent heat flux (LHF) at the surface (Q_L) calculated from the measured profile using equation (13) is shown in Figure 8. For comparison, the LHF based on the Monin-Obukhov surface layer theory as for instance used in the snowpack model SNOWPACK [*Lehning et al.*, 2002] is also shown. In most cases, the LHF is smaller downstream (P2) than upstream (P0). For experiments without drifting snow, this is caused by saturation of the air due to surface sublimation. Interestingly, the reduction of the LHF between the two profiles is larger for experiments with drifting snow. This shows that the saturation effect is stronger when drifting snow is present, reducing surface sublimation. This is in agreement with other studies and would support our finding on the sublimation effect. In nature, this reduction of sublimation from the surface is overcompensated by the drifting snow sublimation from particles originating from the surface. In the wind tunnel and in the beginning of a drifting snow event, the total surface layer LHF (surface LHF plus drifting snow sublimation) is much larger than the surface sublimation without drifting snow. However, because of saturation of the surface layer, the total LHF will decrease with time. Model results by *Bintanja* [2001] even suggested that the total LHF might become smaller than the

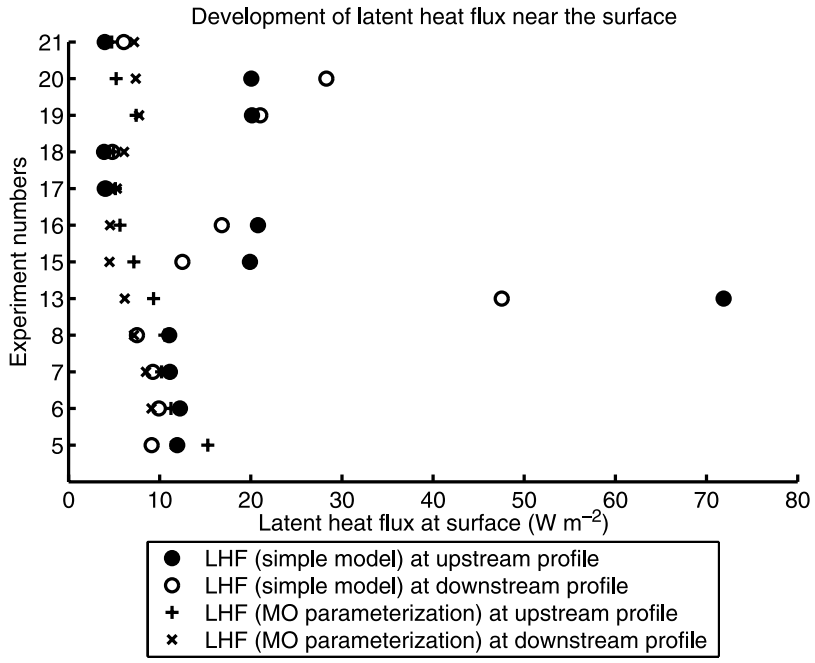

Figure 8. Latent heat flux (LHF) at the upstream (solid circles and pluses) and downstream (open circles and crosses) profile at the surface. On the vertical axes, the various experiments are shown for which simulations were done. The solid and open circles show the LHF as calculated out of the model output using the flux profile relation (equation (13)). For comparison, the plus signs and crosses show the LHF based on the Monin-Obukhov surface layer theory (see text).

surface LHF without drifting snow, which is not supported by our results.

6. Conclusions

[53] Experiments carried out by *Thorpe and Mason* [1966] were the first to measure the sublimation of snow particles surrounded by air. The experiments we present here are the first we are aware of that include measurements of the sublimation rate of an ensemble of particles over a real snow surface. This mirrors conditions found in nature and is useful for studying the upscaling of single-particle processes to those occurring in an ensemble.

[54] Our measurements were made using relatively crude and simple instruments, and some measurements failed. As a result of this, our ability to identify the influence of different environmental forcing is limited. We offer some suggestions to any researcher wishing to attempt further, similar measurements. First, the highest possible sublimation rate is required to give a clear signal over and above the accuracy of the sensors used. This can be achieved by maximizing the number of drifting particles in the tunnel. Secondly, the total sublimation between two measurement arrays can be increased by decreasing wind speeds to increase particle residence time in the control volume. Independent measurements of the snow surface temperature and latent heat flux will help reduce uncertainties during the modeling process. Experiments without a snow surface might give helpful comparison data, although the dynamics of the saltation and suspension process may change over a solid floor, compared to a snow surface [*Clifton and Lehning*, 2008]. Another significant source of uncertainty when comparing results from the model with experiments are the SPCs. We suggest that future improvements in the estimation of the sublimation of drifting snow will be coupled to improvements in SPC technology. The results of our experiments show that quantifying the total experimental error for these type of experiments, for instance by performing multiple replicates of some experiments, is important.

[55] These experiments show that the physics which describe the transfer of heat and water vapor from a single particle, can be transferred to an ensemble of particles. The results obtained from simulations are similar to those seen in a wind tunnel, and show that forcing by solar radiation may increase sublimation up to 50% compared to a nighttime case. This may be for example a significant influence on mass balance in polar regions, or an important factor in the deposition of snow in lee slopes in mountainous environments during a drifting snow event.

[56] Our relatively simple model can be combined with more detailed models of the snow surface [e.g., *Lehning et al.*, 2002], topology and wind fields [e.g., *Raderschall et al.*, 2008] to give improved predictions of the transport of water around alpine terrain. In particular, we have now a basis for implementing snow drift sublimation in our drifting snow model Alpine3D [*Lehning et al.*, 2008; *Raderschall et al.*, 2008], which can be extended to include moisture and temperature feedback from sublimation by solving the coupled particle concentration, moisture and humidity equations.

[57] **Acknowledgments.** This work has partially been financed by the Swiss National Science Foundation. Many people helped build and operate the CES wind tunnel in Shinjo. We especially thank Takeshi Sato, Hiroyuki Hirashima, and the technical staff for on-site and moral support during our experimental work. We also thank Jakob Rhyner, the SLF technical staff, and Carleen Tijm-Reijmer from the Institute for Marine and Atmospheric

Research, Utrecht, Netherlands, for support. Finally, we acknowledge the three anonymous reviewers for their constructive comments.

References

Bintanja, R. (2000), Snowdrift suspension and atmospheric turbulence. Part I: Theoretical background and model description, *Boundary Layer Meteorol.*, *95*, 343–368.

Bintanja, R. (2001), Modelling snowdrift sublimation and its effect on the moisture budget of the atmospheric boundary layer, *Tellus, Ser. A*, *53*(2), 215–232.

Bowling, L., J. Pomeroy, and D. Lettenmaier (2004), Parameterization of blowing-snow sublimation in a macroscale hydrology model, *J. Hydrometeorol.*, *5*, 745–762.

Clifton, A., and M. Lehning (2008), Improvement and validation of a snow saltation model using wind tunnel measurements, *Earth Surf. Processes Landforms*, *33*, 2156–2173.

Clifton, A., J.-D. Rüedi, and M. Lehning (2006), Snow saltation measurements in a drifting-snow wind tunnel, *J. Glaciol.*, *52*(179), 585–596.

Déry, S., and M. Yau (1999), A bulk blowing snow model, *Boundary Layer Meteorol.*, *93*, 237–251.

Déry, S., P. Taylor, and J. Xiao (1998), The thermodynamic effects of sublimating, blowing snow in the atmospheric boundary layer, *Boundary Layer Meteorol.*, *89*, 251–283.

Doorschot, J., N. Raderschall, and M. Lehning (2001), Measurements and one-dimensional model calculations of snow transport over a mountain ridge, *Ann. Glaciol.*, *32*(1), 153–158.

Gordon, M., and P. Taylor (2009), Measurements of blowing snow, part I: Particle shape, size distribution, velocity, and number flux at Churchill, Manitoba, Canada, *Cold Reg. Sci. Technol.*, *55*, 63–74.

Kosugi, K., T. Sato, and A. Sato (2004), Dependence of drifting snow saltation lengths on snow surface hardness, *Cold Reg. Sci. Technol.*, *39*, 133–139.

Lee, L. (1975), Sublimation of snow in a turbulent atmosphere, Ph.D. thesis, Univ. of Wyo., Laramie.

Lehning, M., P. Bartelt, B. Brown, and C. Fierz (2002), A physical SNOWPACK model for the Swiss avalanche warning. Part III: Meteorological forcing, thin layer formation and evaluation, *Cold Reg. Sci. Technol.*, *35*, 169–184.

Lehning, M., H. Löwe, M. Ryser, and N. Raderschall (2008), Inhomogeneous precipitation distribution and snow transport in steep terrain, *Water Resour. Res.*, *44*, W07404, doi:10.1029/2007WR006545.

Liston, G., and M. Sturm (1998), A snow-transport model for complex terrain, *J. Glaciol.*, *44*(148), 498–516.

Mann, G. (1998), Surface heat and water vapour budgets over Antarctica, Ph.D. thesis, Environ. Cent., Univ. of Leeds, Leeds, U. K.

Marty, C. (2000), Surface radiation, cloud forcing and greenhouse effect in the Alps, Ph.D. thesis, Swiss Fed. Inst. of Technol., Zurich, Switzerland.

McDonald, J. (1963), Use of electrostatic analogy in studies of ice crystal growth, *Z. Angew. Math. Phys.*, *14*, 610–619.

Raderschall, N., M. Lehning, and C. Chär (2008), Fine-scale modeling of the boundary layer wind field over steep topography, *Water Resour. Res.*, *44*, W09425, doi:10.1029/2007WR006544.

Schmidt, R. (1982), Vertical profiles of wind speed, snow concentration and humidity in blowing snow, *Boundary Layer Meteorol.*, *23*, 223–246.

Stull, R. B. (1989), *An Introduction to Boundary Layer Meteorology*, 2nd ed., 666 pp., Kluwer Acad., Dordrecht, Netherlands.

Thorpe, A., and B. Mason (1966), The evaporation of ice spheres and ice crystals, *Br. J. Appl. Phys.*, *17*, 541–548.

A. Clifton, M. Lehning, and J.-D. Rüedi, WSL Swiss Federal Institute for Snow and Avalanche Research, Fluelastrasse 11, Davos CH-7260, Switzerland.

M. Nemoto, A. Sato, and S. Yamaguchi, Snow and Ice Research Center, National Research Institute for Earth Science and Disaster Prevention, Nagaoka 940-0821, Japan.

K. Nishimura, Department of Environmental Science, Faculty of Science, Niigata University, Karashi, Niigata 950-2181, Japan.

N. Wever, Royal Netherlands Meteorological Institute, P.O. Box 201, NL-3730 AE, De Bilt, Netherlands. (nander.wever@knmi.nl)